Extraction of Rooftops from LiDAR and Multispectral Imagery

Angela M. Kim[1,2], Fred A. Kruse[1,2], Richard C. Olsen[1,2], Chris C. Clasen[2]

Physics Department[1], Remote Sensing Center[2], Naval Postgraduate School, 833 Dyer Rd., Monterey, CA, USA

amkim@nps.edu, fakruse@nps.edu, olsen@nps.edu, ccclasen@nps.edu

Abstract: A rooftop extraction scheme based on statistical analysis of the LiDAR point cloud is presented. Spectral data are incorporated to reduce false alarms due to vegetation and to provide spectral discrimination of rooftop materials.

OCIS codes: (280.3640) Lidar; (280.4788) Optical sensing and sensors

1. Introduction

The results presented here are part of a larger project investigating methods for extracting information from remotely sensed data that are meaningful to city planners and emergency responders for disaster planning and emergency response efforts. LiDAR data provide an excellent means of detecting rooftops in a scene by exploiting spatial statistics of the point cloud data. If post-event LiDAR data are available for comparison, these methods will be useful for post-event damage assessment. The process can be semi- or fully-automated. Most false detections are due to vegetation in the scene. Incorporation of spectral data allow calculation of the Normalized Difference Vegetation Index (NDVI) [1], which eliminates the majority of false rooftop detections present if the LiDAR data are processed singly. Incorporation of the spectral data requires orthorectification and introduces some errors due to temporal and spatial resolution mismatches. Combined analysis of the LiDAR and multispectral data also aids in improved separation of specific types of rooftop materials from spectrally similar non-rooftop areas.

2. Study Area and Data Collection Parameters

The study area incorporates the city of Monterey, CA, USA, and includes typical classes of an urban scene. Airborne LiDAR data collected with an ALTM Gemeni system and spectral data from the WorldView-2 (WV-2) satellite are used in the rooftop extraction approach. National Agriculture Imagery Program (NAIP) 1-m orthophotos collected in 2010 are used to verify results. LiDAR data collected in September 2010 consist of classified (ground/non-ground) point clouds in the LAS format. Point density is approximately 2.5 points/m^2, or an average post spacing of 0.63 m. LiDAR were collected with the following settings:

- System PRF: 100 kHz
- Scan Frequency: 40 Hz
- Scan Angle: +/- 25 degrees
- Laser Wavelength: 1064 nm
- Swath: 887.75 m
- Flightline Overlap: 50%

WV-2 spectral data collected on 15 April 2011 were orthorectified using ground control points taken from GIS layers provided by the City of Monterey, and a 10m DEM from the US Geological Survey. Accuracy of the orthorectified image product was measured to be +/- 3.2 m. The data have pixel sizes of 2.0x2.2 m.

3. LiDAR Data Processing

3.1. Statistics of Local Neighborhoods and Extraction of Flat Surfaces

A grid of query points is defined covering the (x,y) extent of the LiDAR data with a spacing between points based on a user-defined grid-size. For the study area, the post spacing of the LiDAR data is approximately 0.63 m, so the grid-size was set slightly larger (at 1 m). A local neighborhood is defined around each grid point so that the LiDAR (x,y) data space is completely covered by neighborhoods with no gaps. Choosing a grid-size slightly larger than the post spacing ensures multiple points are located within most local neighborhoods, which is necessary for meaningful statistics. The standard deviation of the vertical distribution of LiDAR points within each local neighborhood is calculated. A raster image is created by storing the value of the statistic at each grid point.

For flat surfaces, such as the ground or manmade structures, the standard deviation of elevation values within a local neighborhood is low as compared to that of vegetated areas. Therefore, a threshold can be defined to distinguish the flat surfaces from vegetated areas. Setting this threshold is subjective, but the overall process is robust enough that the choice is not overly critical. Means for automating the choice of this value will be investigated at a later date.

3.2. Ground Masking

A mask to exclude ground areas is created by marking any of the gridded query points which have a LiDAR point classified as being a ground return within the local neighborhood. The mask created by this process is useful, but the result is noisy. A morphological erosion filter is used to remove noise from the masked result.

In this study, the ground mask is based on the classification of LiDAR points provided by the vendor. The specifics of the scheme used to classify ground points were unavailable, and this represents a degree of uncertainty in the reproducibility of results using other data sets. An investigation of different methods for classifying ground returns, and the effects of this on the rooftop extraction process, will be made at a later date.

3.3. Vegetation Masking Based on LiDAR Return Number

When a LiDAR pulse is emitted, it may be scattered and reflected off of multiple surfaces, causing multiple returns to be detected for a single pulse of emitted energy. For vegetation or other rough surfaces, there is a high likelihood of multiple returns being detected. A mask that excludes neighborhoods having multiple returns is useful for masking some of the vegetated areas. This mask, however, excludes returns from vegetation that happen to be first or single returns. A morphological closing filter is used to fill in some of the smaller gaps in the vegetation mask image.

3.4. Shingle Roof Exceptions

In the LiDAR data, shingle roofs (and other dark asphalt surfaces) show up as gaps in the data. These surfaces are not reflective enough at the LiDAR wavelength to be detected. These locations can be mapped by finding grid points that do not have any LiDAR points in their local neighborhood. To separate gaps due to shingle roofs from the gaps due to asphalt roads or parking lots, a threshold based on component size excludes any components larger than 30 m^2. A second threshold excludes "long and skinny" components by measuring the ellipticity of a bounding ellipse drawn around the component. This excludes most of the highway areas, while retaining most of the shingle roof areas.

3.5. Removal of False Detections

A final LiDAR processing step uses a threshold based on component size to exclude objects that are too small to be buildings ($<$10 m^2). Some false detections are inevitable due to healthy vegetation in the scene. Results of the rooftop extraction using only the LiDAR point cloud data are shown in the middle row of Fig. 1.

4. Spectral Data Processing

A vegetation map is created using a thresholded WV-2 NDVI result. Definition of the threshold is subjective, but only healthy vegetation is dense enough to be confused with flat surfaces in the LiDAR processing. Choosing an NDVI threshold value of 0.24 safely maps the healthy vegetation in the scene, with few non-vegetation blunders. Incorporating spectral data in the rooftop extraction process allows removal of a large portion of the false detections, producing a fairly reliable roof map. Results of the rooftop extraction using both LiDAR and spectral data are shown in the bottom row of Fig. 1. The LiDAR extracted rooftops can be used to mask the WV-2 data, eliminating spectrally similar non-rooftop materials (Fig. 2). There are challenges in dealing with the spectral data, however, including the need for the accurate orthorectification, and the possibility of errors due to temporal and spatial resolution mismatches.

5. Results of Rooftop Extraction and Analysis

Image chips from a 1-m NAIP orthophoto shown in the top row of Fig. 1 provide a visual comparison of rooftop extraction results. Larger buildings are outlined fairly accurately, while the edges of smaller residential buildings are sometimes less clear. The inclusion of spectral imagery tends to reduce some of the false alarms due to vegetation present in the LiDAR-only results. The false alarms which are removed by including spectral imagery are highlighted in red in the bottom row of Fig. 1.

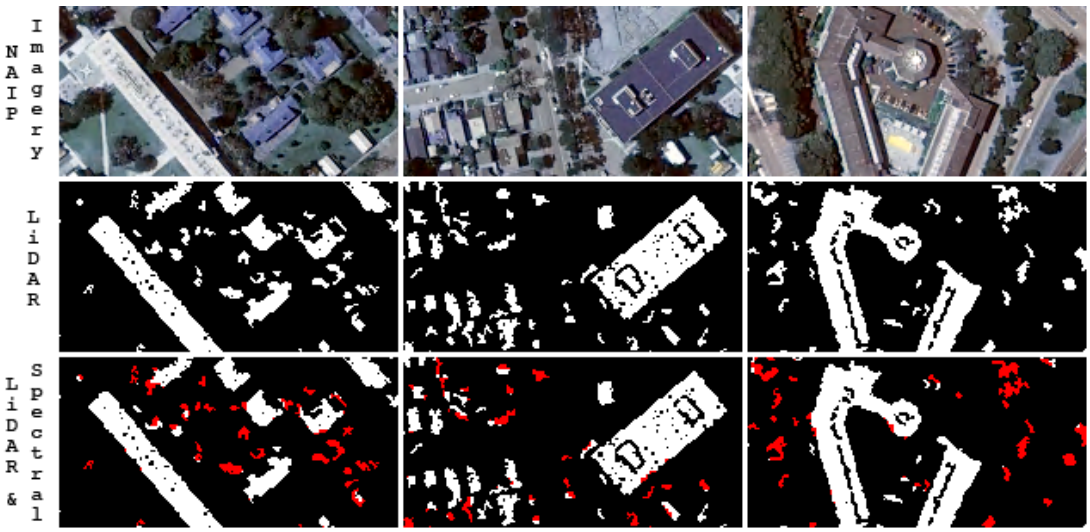

Fig. 1. (Top) NAIP orthophoto; (Middle) LiDAR-only rooftop extraction result; (Bottom) Rooftop extraction result using LiDAR and WV-2 spectral data shown in white; false alarms in the LiDAR-only result which are removed by including the spectral data are shown in red.

Fig. 2. (Left) WV-2 true color image showing selected buildings with red-tile roofs and spectrally similar red tennis courts. (Right) Combined LiDAR rooftop extraction result and WV-2 true color image. Note that the spectrally similar (non-rooftop) tennis courts have been removed along with other materials such as vegetation and paved areas.

6. Conclusions and Future Work

The methods presented here are effective for extracting rooftops from LiDAR point cloud data. Using LiDAR alone, a rooftop map can be created which contains false alarms due to vegetation. Incorporation of spectral data presents some challenges, but can be very useful for removing false alarms due to vegetation. Masking the spectral data using the rooftop extraction enables analysis of rooftop materials. Further work is needed to verify the methods using different data, to automate the definition of threshold values, and to fully exploit the potential of the spectral data. The output of the current process can be used as a mask for the LiDAR point cloud to classify and extract returns from buildings, enabling the creation of 3D building models.

7. Acknowledgements

This research was partially supported by the Science and Technology Directorate, USA Department of Homeland Security (DHS). The LiDAR data were provided by the Association of Monterey Bay Area Governments (AMBAG), via a USGS grant through the American Reinvestment and Recovery Act of 2009. WV-2 data were provided by the National Geospatial-Intelligence Agency (NGA) under the NextView imagery license agreement.

References

1. C.J. Tucker. “Red and photographic infrared linear combinations for monitoring vegetation,” Rem. Sens. Environ., **8**, 127–150 (1979).